EPS-paper 370
July 2003

A Scalar Top Study with c-Quark Tagging at a Linear e^+e^- Collider

A. Finch[1], H. Nowak[2], A. Sopczak[1]
[1] *Lancaster University, United Kingdom*
[2] *DESY Zeuthen, Germany*

Abstract

The potential to discover a scalar top quark has been studied for the TESLA project at $\sqrt{s} = 500$ GeV. Background process were simulated for the equivalent of an integrated luminosity of at least $1000\,\mathrm{fb}^{-1}$. The detector response has been simulated with the SIMDET detector description which includes a charge coupled device (CCD) vertex detector. For a 180 GeV scalar top the selection efficiency has been optimized with an Iterative Discriminant Analysis (IDA). Good agreement with previous results based on an SGV simulation was found and the expected sensitivity is enhanced with the application of c-quark tagging which takes advantage of the additional information provided by the vertex detector. The use of two beam polarization configurations allows the scalar top mixing angle mass to be deduced from two independent cross section measurements. Using the latest estimation of the beam polarization parameters at TESLA, and a 180 GeV scalar top at minimum production cross section, gives an error of $\Delta m_{\tilde{t}_1} = -0.74/+0.69$ GeV on the mass and $\Delta\cos\theta_{\tilde{t}} = -0.0053/+0.0058$ on the mixing angle when using charm tagging. The MSSM parameters for the Snowmass point 5[13] at $\cos\theta_{\tilde{t}} = 0.513$ predict a scalar top of 210 GeV and a neutralino of about 120 GeV. For this parameter choice $\Delta m = -0.33/+0.31$ GeV and $\Delta\cos\theta_{\tilde{t}} = -0.0049/+0.0053$ is obtained when using charm tagging.

Contributed Paper for EPS (Aachen)

1 Introduction

The study of the scalar top ('stop') quark is of particular interest, since the lighter stop mass eigenstate is likely to be the lightest scalar quark in a supersymmetric theory. The mass eigenstates are $m_{\tilde{t}_1}$ and $m_{\tilde{t}_2}$ with $m_{\tilde{t}_1} < m_{\tilde{t}_2}$, where $\tilde{t}_1 = \cos\theta_{\tilde{t}}\tilde{t}_L + \sin\theta_{\tilde{t}}\tilde{t}_R$ and $\tilde{t}_2 = -\sin\theta_{\tilde{t}}\tilde{t}_L + \cos\theta_{\tilde{t}}\tilde{t}_R$. In this paper the possibilities to detect stop quarks at a high-luminosity e^+e^- linear collider like the TESLA project [1] are studied. In a previous study [2] the discovery potential for scalar top quarks was simulated for $\sqrt{s} = 500$ GeV and an integrated luminosity of $500\,\mathrm{fb}^{-1}$ using Iterative Discriminant Analysis (IDA) [3]. Using the results of that study it was shown that high precision measurements could be made of the mass and mixing angle for benchmark stop parameters [4]. In the previous studies, charm tagging variables were not available in the simulation. As the signal process contains charm quarks while the backgrounds largely do not, it is expected that the inclusion of charm tagging will improve the signal to background ratio. This paper repeats the previous analysis using a new simulation which has charm tagging included to measure the improvement that can be achieved. In addition the effect of beam polarization is considered, and the possibilities of measuring the stop at 'Snowmass Point 5' are explored.

2 Event Simulation

The simulated signal process is $e^+e^- \to \tilde{t}_1\bar{\tilde{t}}_1$, where subsequently each scalar top decays into a c-quark and a neutralino which escapes detection. The resulting signature is the presence of events containing two charm jets and large missing energy. This channel is dominant unless the decay into a chargino is kinematically allowed. The signal generator [5] includes initial state radiation and beamstrahlung. The generated events are passed through the SIMDET detector simulation [6]. The previous analysis was based on the SGV detector simulation [7]. As the detector design has changed so as to give larger coverage in the forward region, and the simulation program is more sophisticated, the results of this analysis are expected to be similar but not identical to the previous one. A 180 GeV scalar top and a 100 GeV neutralino are simulated. Figure 1 shows distributions simulated with SGV and SIMDET. It can be seen that small differences exist between the two simulations. For this study the number of background events is more than doubled compared to the previous study, however, to simplify comparison to the previous work, all rates are given for an integrated luminosity of $500\,\mathrm{fb}^{-1}$.

Figure 1: Distributions for stop quarks after preselection simulated by the SGV and SIMDET programs for $m_{\tilde{t}_1} = 180$ GeV and $m_{\tilde{\chi}^0} = 100$ GeV.

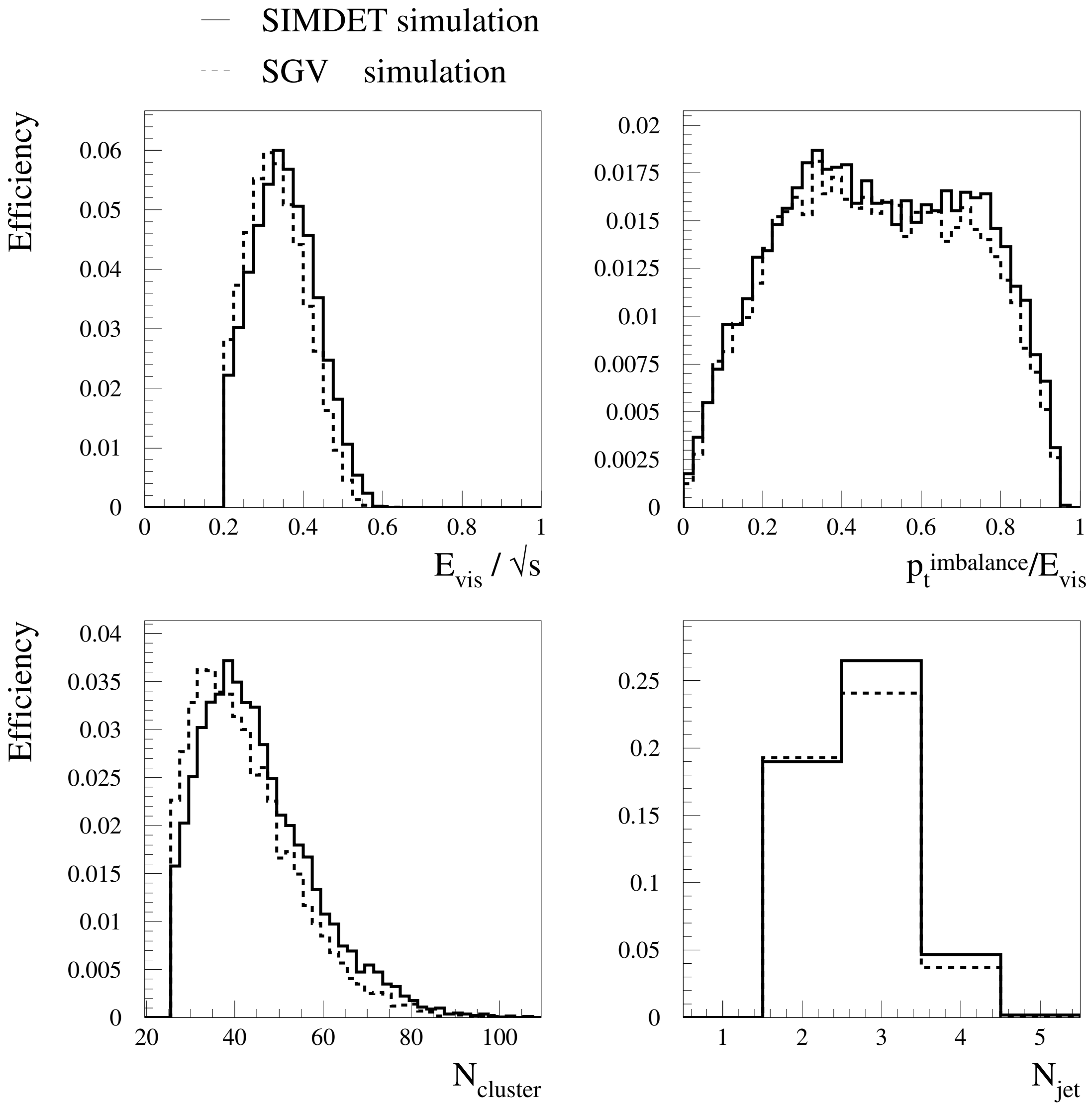

Table 1: Number of simulated signal and background events before and after the preselection.

Events	Channel						
	$\tilde{\chi}^0 c \tilde{\chi}^0 \bar{c}$	$q\bar{q}$	WW	eWν	$t\bar{t}$	ZZ	eeZ
Generated (1000s)	50	13,410	7,870	5,729	850	680	6,690
Expected (1000s) in 500 fb^{-1}		6,025	3,930	2,792	287	300	3,000
Expected in 500 fb^{-1} after presel.	48%	53,762	90,599	246,571	31,721	1393	12,641

3 Event Preselection

The event selection consists of several steps. First, an event preselection is applied using the hadronic character and large missing energy of the simulated signal. The following preselection cuts, which are identical to those in the previous study are applied: $25 < N_{\text{cluster}} < 110$, $0.2 < E_{\text{vis}}/\sqrt{s} < 0.7$, $E_{||}^{\text{imbalance}}/E_{\text{vis}} < 0.5$, thrust < 0.95, $|\cos\theta_{\text{thrust}}| < 0.7$. At this stage similar fractions of events survive in the signal and background channels as in the previous analysis.

The number of simulated events for the signal and for each background channel, the number of expected events for each background, and the number of remaining events after the preselection, are given in Table 1.

4 Iterative Discriminant Analysis

In order to separate the signal from the background, the following selection variables are defined: visible energy, number of jets, thrust value and direction, number of clusters, transverse and parallel momentum imbalance, acoplanarity and invariant mass of the two highest energy jets. In addition to these variables, which were defined for the previous analysis, a charm tag is introduced. The inputs for the construction of the charm tag come from the program ZVTOP [8]. These are used as input to a neural network [9] which is trained to identify charm jets using simulated Z events. This results in a variable that is close to 1 for a jet originating with a charm quark, and close to 0 otherwise, as shown in Fig. 2 (c) and (d).

Figure 2 shows the simulated visible energy divided by $\sqrt{s}$ and the transverse momentum imbalance as a fraction of the visible energy, for events after the preselection. After applying the further selection $E_{\text{vis}}/\sqrt{s} < 0.52$, and $N_{\text{cluster}} < 80$, 271,408 background events remain, compared to 278,377 previously. From this point the analysis is performed twice, once without the charm tag, to allow comparison with the previous analysis, and once with the charm tag to measure to what extent this improves the signal to background ratio. Half of the preselected background events and half of the preselected signal events are used to train the IDA. The training results in a weight, designated IDA_1, for each event that can be used to select a sample with an increased signal fraction. Figures 3 and 4 show the IDA output for all preselected events and the thrust value for those events with IDA_1 greater than zero, which is defined so as to select 50% of the signal. Applying this selection to the backgrounds leaves 7500 events when no charm tagging is used, and 4200 events when it is.

The events which have IDA_1 > 0 are passed through the IDA program a second time. Figure 5 shows the second IDA output variable (IDA_2), which is again normalised so that 50% efficiency occurs at IDA_2 $= 0$ and the resulting number of background events as a function of the signal efficiency for the case without charm tagging, while Fig. 6 shows the improvement that is obtained by including charm tagging. The maximum efficiency is 25% due to reduction of the signal by approximately 50% at the preselection stage, and again after the first stage of the IDA. For 12% efficiency, 300 background events are expected in $500\,\text{fb}^{-1}$, compared to 400 in the previous analysis, whereas 100 background events are expected at this efficiency when charm tagging is used.

Figure 2: Distributions for background and signal events after preselection. (a) Visible energy as a fraction of $\sqrt{s}$. (b)Transverse momentum imbalance. (c) Charm tag for most energetic jet. (d) Charm tag for second most energetic jet.

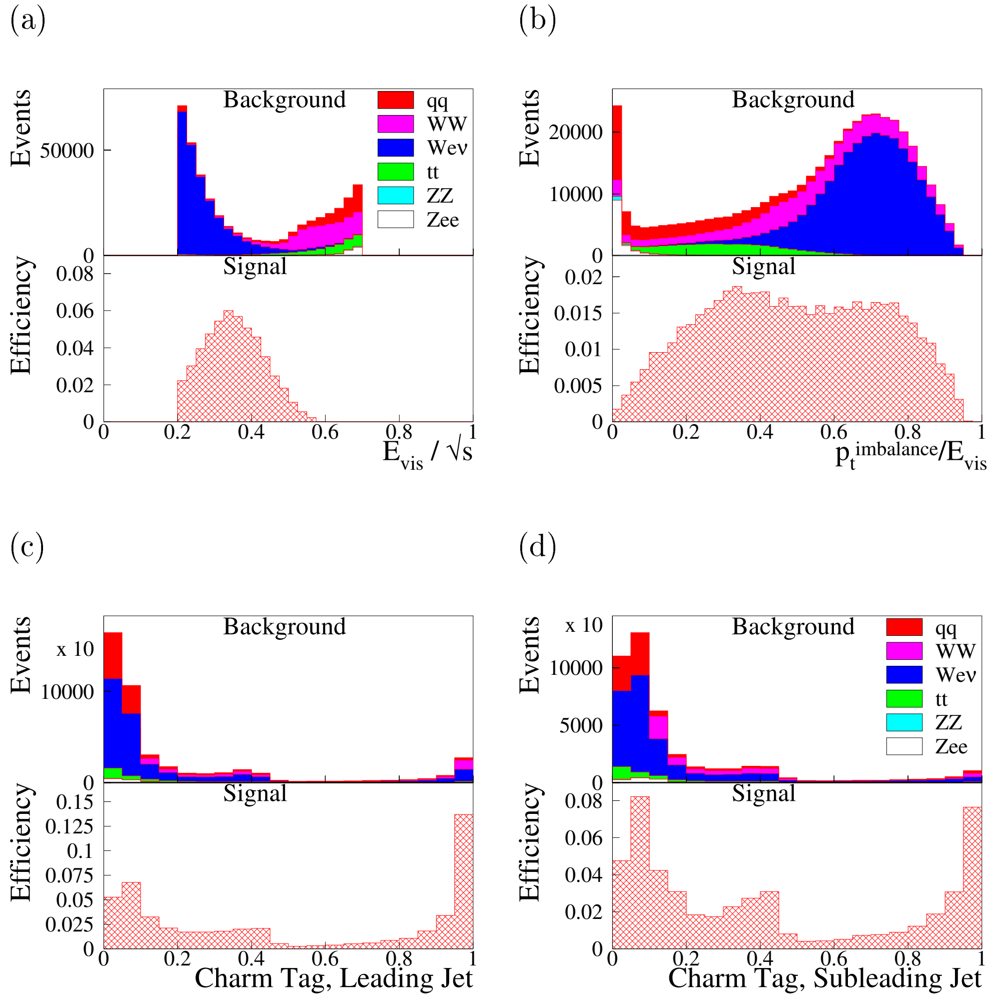

Figure 3: (a) Output from first stage of IDA program (IDA_1). (b) Thrust for events with IDA_1 greater than zero.

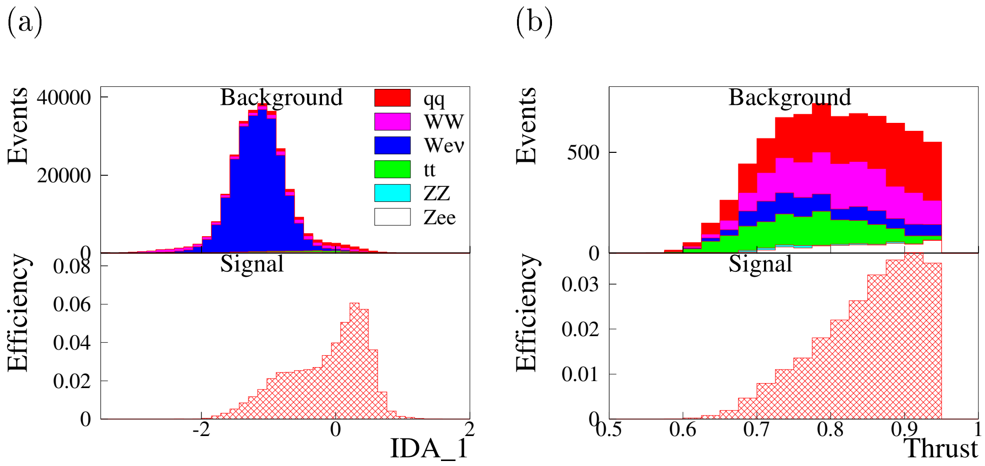

Figure 4: As Figure 3 with charm tagging variables also used in the IDA program.

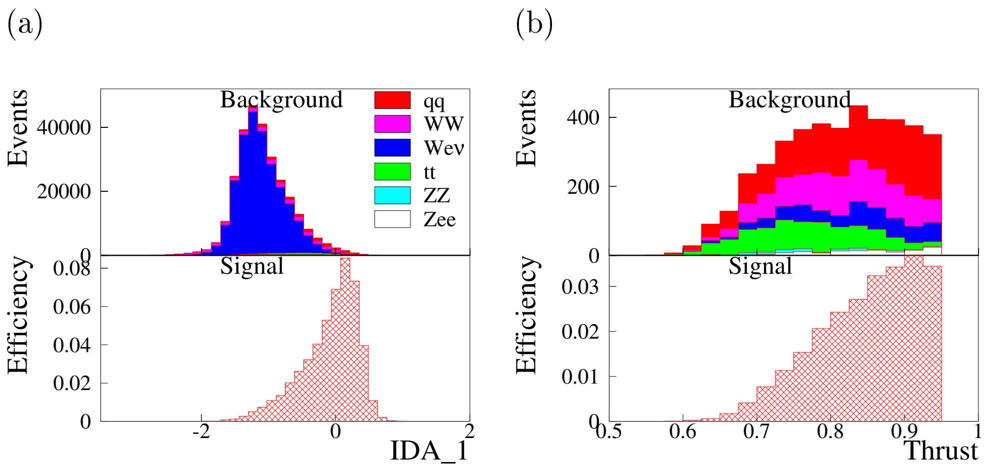

Figure 5: (a) Output from second stage of IDA. (b) Number of signal and background events versus efficiency for a 180 GeV scalar top and a 100 GeV neutralino. (Charm tagging information not used)

(a) (b)

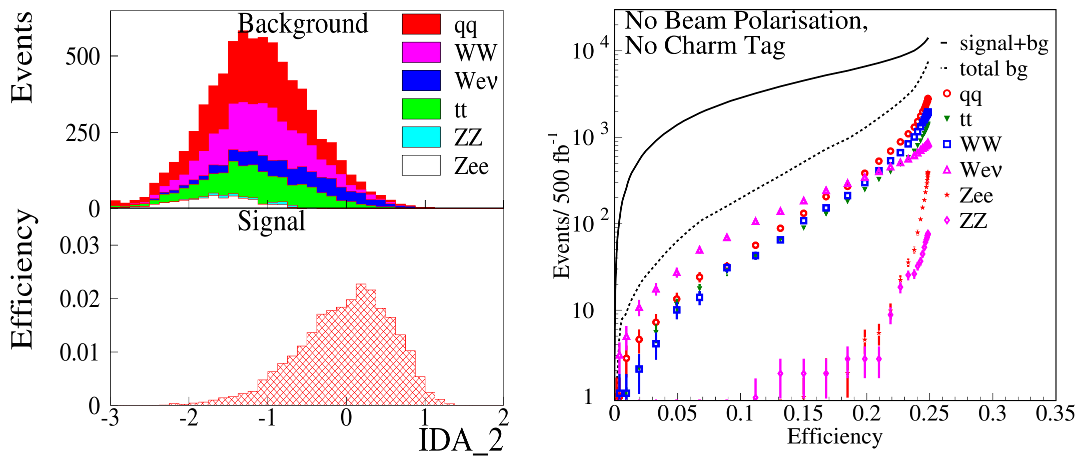

Figure 6: As Fig. 5 with charm tagging information used.

(a) (b)

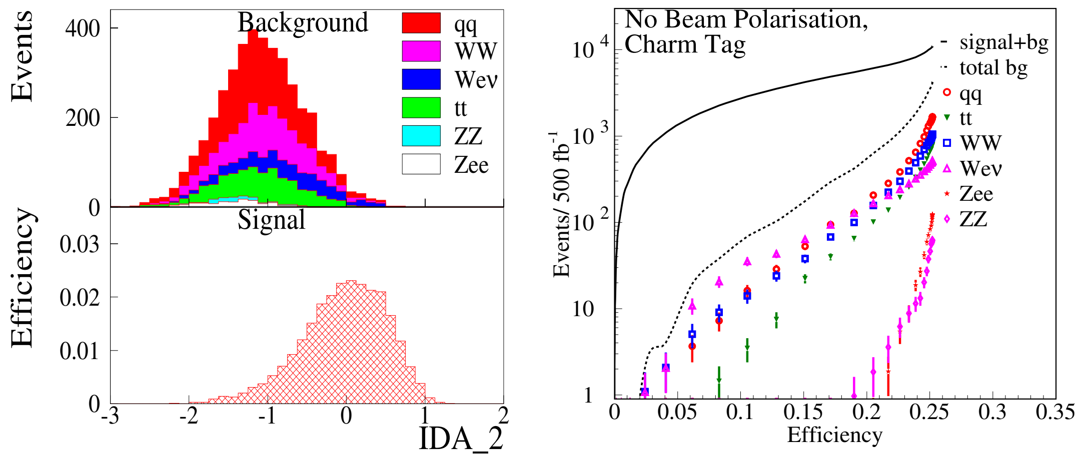

Pol. of e^-	Pol. of e^+	$\tilde{t}_1\bar{\tilde{t}}_1$ CALVIN	Weν GRACE	WW WOPPER	$q\bar{q}$ HERWIG	$t\bar{t}$ HERWIG	ZZ COMPHEP
−0.8	0.6	0.0818	10.7	22.6	21.5	1.11	0.909
0	0.0	0.0535	5.59	7.86	12.1	0.574	0.864
0.8	−0.6	0.0764	1.78	0.786	13.0	0.542	0.464

Table 2: Signal and background cross sections (pb) from different event generators for e^- and e^+ polarization states ($m_{\tilde{t}_1} = 180$ GeV and $\cos\theta_{\tilde{t}} = 0.57$). The Zee cross section is 0.6 pb.

5 Beam Polarization

The polarization of the e^+ and e^- beams at a future linear collider offers the opportunity to enhance or suppress the left- or right-handed couplings of the scalar top signal and to determine mass and mixing angle independently. The production cross section of each background process depends differently on the polarization. It is therefore important for a high-statistics analysis to study the expected background channels individually. The expected cross sections [10, 11] are given in Table 2 for different beam polarization states. The background rates were recalculated for a machine polarization of $-0.8/+0.6$ (left-polarization) and $+0.8/-0.6$ (right-polarization) as a function of the signal efficiency [12]. The results are shown in Fig. 7.

Figure 8 shows the corresponding error bands and the error ellipse in the $m_{\tilde{t}_1}$ – $\cos\theta_{\tilde{t}}$ plane with and without charm tagging for 0.8/0.6 left- and right-polarization of the e^-/e^+ beams and a luminosity of 500 fb^{-1} each. Detailed results are given in Table 3. The highest statistical precision is obtained when using charm tagging giving an error of $\Delta m_{\tilde{t}_1} = -0.74/+0.69$ GeV for $m_{\tilde{t}_1} = 180$ GeV and $\Delta\cos\theta_{\tilde{t}} = -0.0053/+0.0058$.

Snowmass Point 5

At the Snowmass 2001 "Summer Study on the Future of Particle Physics" a consensus was reached about a number of defined mSugra points. One of them is dedicated to a light scalar top [13]. For this point the parameters $m_0 = 150$ GeV, $m_{1/2} = 300$ GeV, $A_0 = -1000$, $\tan\beta = 5$ and $\mu > 0$ generate a light scalar top at 210 GeV with a mixing angle of $\cos\theta_{\tilde{t}} = 0.513$ and a neutralino of 121.2 GeV mass (SUSYGEN [14]). The scalar top decays at 100% into $\tilde{\chi}^0$c because the chargino mass is about 10 GeV higher than the scalar top mass. A three-particle decay of the scalar top into b–lepton–sneutrino is also excluded because the sneutrino mass is too high.

Figure 7: Number of signal and background events versus efficiency for a 180 GeV scalar top and a 100 GeV neutralino with left and right handed beam polarizations. For lots in the top row charm tagging has been used, while for those in the bottom row it has not.

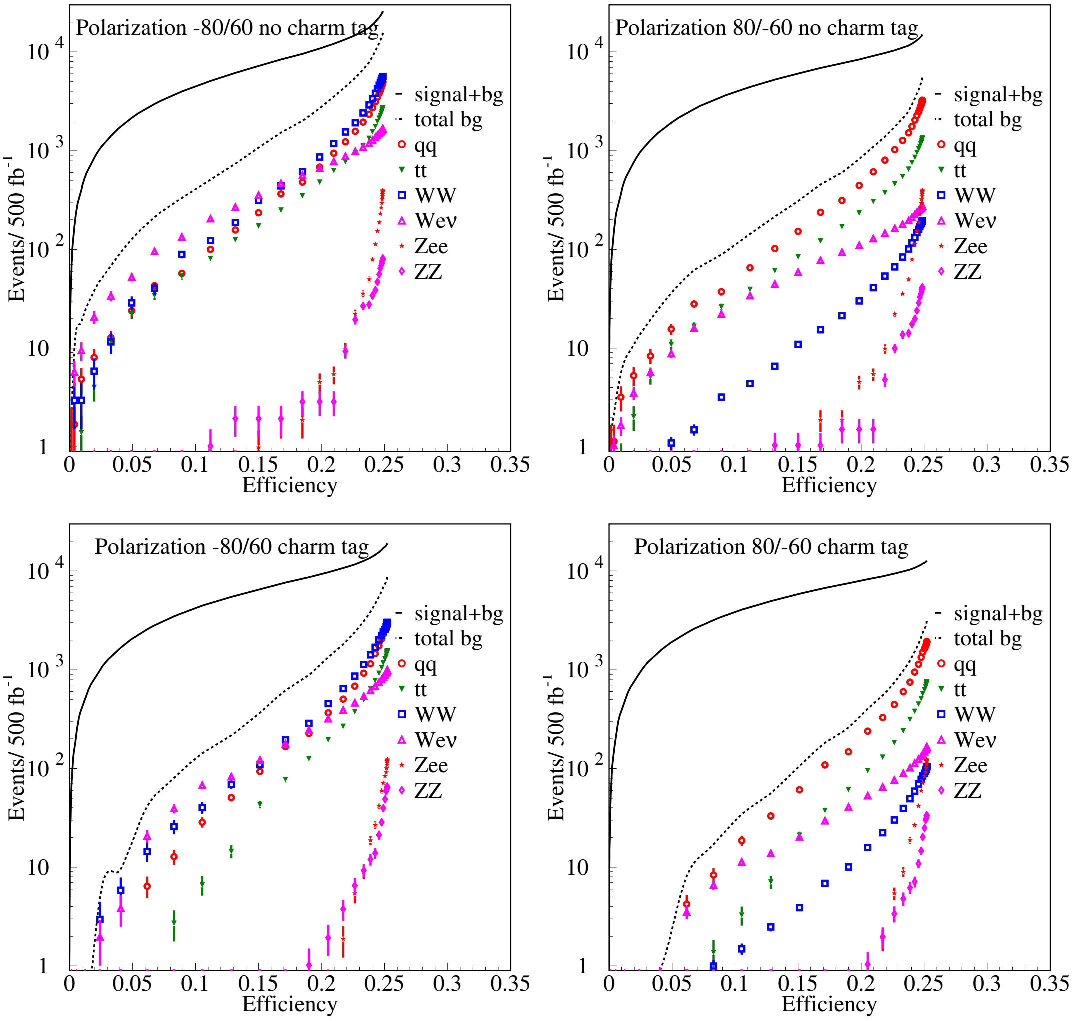

The cross section for the production of a scalar top at 210 GeV and $\cos\theta_{\tilde{t}} = 0.513$ is roughly half of that obtained for a 180 GeV scalar top at minimum cross section. As the mass differences between scalar top and neutralino for both scenarios are roughly the same (80 and 90 GeV, respectively) the same Standard Model backgrounds have been taken into account. Thus, only the number of signal events decreases by about a factor of two.

In this detailed scenario light MSSM particles are the 220 GeV scalar top 1, the 121 GeV neutralino 1, the 223 GeV neutralino 2, the 223 GeV chargino 1, and the 114 GeV Higgs bosons. Therefore, possible SUSY background reactions are:

$e^+e^- \to \tilde{\chi}^0_2\tilde{\chi}^0_1 \to Z\tilde{\chi}^0_1\tilde{\chi}^0_1$	$e^+e^- \to \tilde{\chi}^0_2\tilde{\chi}^0_2 \to Z\tilde{\chi}^0_1 Z\tilde{\chi}^0_1$	$e^+e^- \to \tilde{\chi}^+\tilde{\chi}^- \to W\tilde{\chi}^0_1 W\tilde{\chi}^0_1$
(1a) $\to$ $q\bar{q}\tilde{\chi}^0_1\tilde{\chi}^0_1$	(2a) $\to$ $q\bar{q}\tilde{\chi}^0_1 q\bar{q}\tilde{\chi}^0_1$	(3a) $\to$ $q\bar{q}\tilde{\chi}^0_1 q\bar{q}\tilde{\chi}^0_1$
(1b) $\to$ $\ell^+\ell^-\tilde{\chi}^0_1\tilde{\chi}^0_1$	(2b) $\to$ $q\bar{q}\tilde{\chi}^0_1\ell^+\ell^-\tilde{\chi}^0_1$	(3b) $\to$ $q\bar{q}\tilde{\chi}^0_1\ell\nu\tilde{\chi}^0_1$

Only (1a) has a signature similar to the signal, however, the expected production rate is very small for this channel as $\sigma(e^+e^- \to \tilde{\chi}^0_1\tilde{\chi}^0_2) = 0.037$ pb and the decay branching ratios are $BR(\tilde{\chi}^0_2 \to Z\ \tilde{\chi}^0_1) = 0.012$ and $BR(Z \to q\bar{q}) = 0.70$. Thus, $\sigma(e^+e^- \to \tilde{\chi}^0_1\tilde{\chi}^0_2 \to q\bar{q}\tilde{\chi}^0_1\tilde{\chi}^0_1) = 0.31$ fb and this background rate is expected to be much smaller than the expected signal rate. Therefore, no significant background from Supersymmetric processes is expected. The lower two rows in Table 3, and the lower plots in Fig. 8 show the effect on the resolution on $m_{\tilde{t}_1}$ and $\cos\theta_{\tilde{t}}$ when working with a 210 GeV stop mass.

$m_{\tilde{t}_1}$ (GeV)	Charm Tag	Background (left)	Background (right)	$\Delta\sigma_{\rm left}$ (fb)	$\Delta\sigma_{\rm right}$ (fb)	$\Delta m_{\tilde{t}_1}$ (GeV)	$\Delta\cos\theta_{\tilde{t}}$
180	no	588	166	0.86	0.80	-0.80 / +0.79	-0.0054 / +0.0058
180	yes	183	49	0.83	0.76	-0.74 / +0.69	-0.0053 / +0.0058
210	no	588	166	0.38	0.42	-0.38 / +0.34	-0.0053 / +0.0057
210	yes	183	49	0.35	0.41	-0.33 / +0.31	-0.0049 / +0.0053

Table 3: Expected number of background events, and the resulting errors on the cross section, mass and mixing angle from simulations with and without charm tagging.

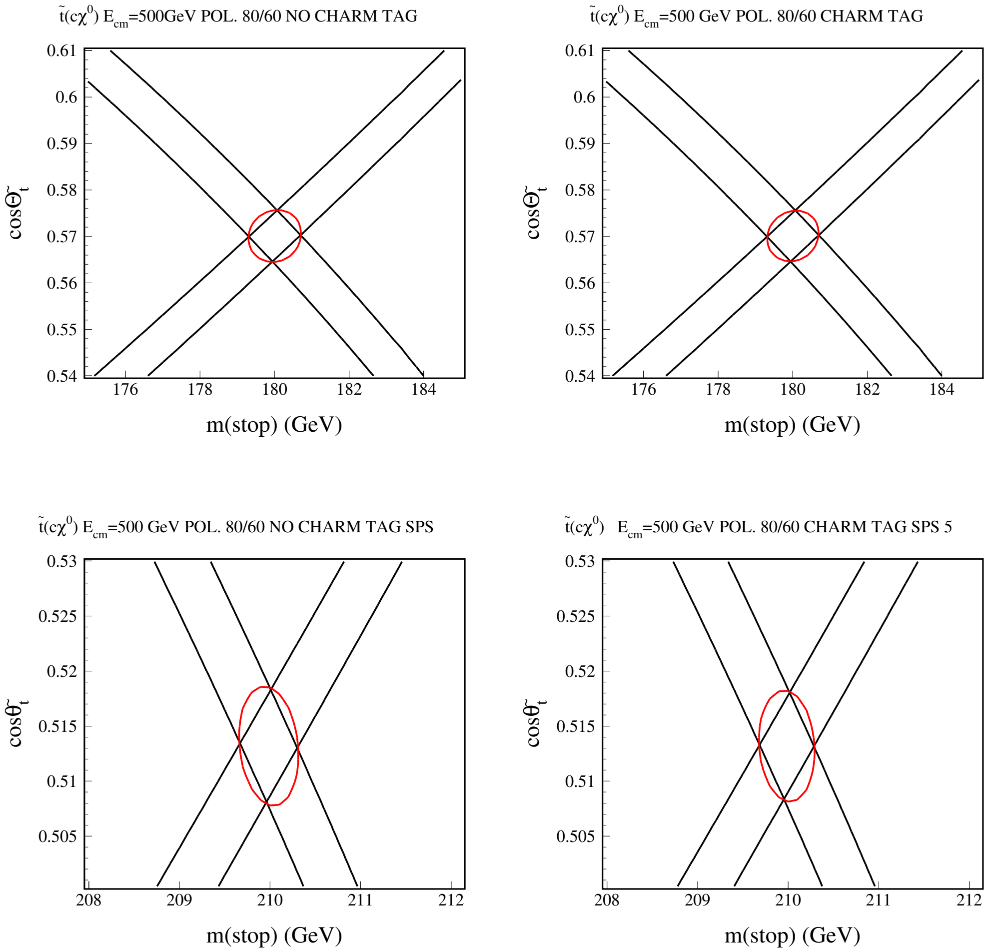

Figure 8: Error bands and the corresponding error ellipse as a function of $m_{\tilde{t}_1}$ and $\cos\theta_{\tilde{t}}$ for $\sqrt{s} = 500$ GeV, $\mathcal{L} = 500$ fb^{-1}. Left: without charm tagging. Right: with charm tagging. Upper row: $m_{\tilde{t}_1} = 180$ GeV. Lower row: $m_{\tilde{t}_1} = 210$ GeV.

6 Conclusion

A study of stop quark production at a linear e^+e^- collider has been performed using events produced with the SIMDET detector simulation and compared to a previous analysis based on the SGV detector simulation. Various distributions have been compared and found to be as similar.Small differences are observed which are expected given the differences in the detector definition between the two studies. The final event selection, based on iterative discriminant analysis predicts a background of 300 events, at 12% efficiency as opposed to 400 events in the previous analysis using the same variables. The background is reduced by a further factor of three when charm tagging variables are also used as inputs to the iterative discriminant analysis. Operating the accelerator in two different polarization configurations allows both the mass and the mixing angle of the stop quark to be deduced from two measurements of the cross section.

A high-luminosity linear collider with an experiment which includes a vertex detector therefore has a great potential for precision measurements in the scalar quark sector predicted by supersymmetric theories.

References

[1] 'Conceptual Design Report of a 500 GeV e^+e^- Linear Collider with Integrated X-ray Laser Facility', DESY 1997-048, ECFA 1997-182.

[2] M. Berggren, R. Keranen, H. Nowak, A. Sopczak, Eur.Phys.J.direct **C2** (2000) 7.

[3] J. Malmgren and K. Johansson, Nucl. Inst. Methods **A 403** (1998) 481.

[4] A. Finch, H. Nowak, A. Sopczak, hep-ph/0211140.

[5] A. Sopczak, in 'Physics at LEP2', CERN 96-01, p. 343.

[6] M. Pohl, H.J. Schreiber, hep-ex/0206009.

[7] M. Berggren, http://home.cern.ch/b/berggren/www/sgv.html

[8] D. J. Jackson, Nucl. Inst. and Meth. **A388**, (1997) 247.

[9] T. Kuhl, proc. Vertex 2002 to appear in Nucl. Inst. Methods .

[10] H. Eberl, A. Bartl, W. Majerotto, Nucl. Phys. **B 472** (1996) 481.

[11] T. Sjostrand, http://www.thep.lu.se/tf2/staff/torbjorn/LCphysgen.html

[12] H. Nowak, A. Sopczak, Proc. Chicago workshop, Oct. 2000; hep-ph/0102341.

[13] N. Ghodbane, H.-U. Martyn, LC-TH-2001-079, hep-ph/02011233.

[14] N. Ghodbane, S. Katsanevas, P. Morawitz, E. Perez, SUSYGEN 3, hep-ph/9909499.